

# Modulated Linear Te-chains in Ba<sub>3</sub>ScTe<sub>5</sub>: Synthesis, Crystal Structure, Optical, Resistivity Studies, and Electronic Structure

Mohd Ishtiyak,<sup>†</sup> Gopabandhu Panigrahi,<sup>†</sup> Subhendu Jana,<sup>†</sup> Jai Prakash,<sup>†,‡</sup> Adel Mesbah,<sup>‡,§</sup> Christos D. Malliakas,<sup>‡</sup> Sébastien Lebègue,<sup>⊥</sup> and James A. Ibers<sup>‡,\*</sup>

<sup>†</sup>Department of Chemistry, Indian Institute of Technology Hyderabad, Kandi, Sangareddy, Telangana 502285, India

<sup>‡</sup>Department of Chemistry, Northwestern University, 2145 Sheridan Road, Evanston, IL 60208-3113, United States

<sup>§</sup>ICSM, Univ Montpellier, CEA, CNRS, ENSCM, Site de Marcoule, Bagnols-sur-Cèze, France

<sup>⊥</sup>Laboratoire de Physique et Chimie Théoriques (LPCT, UMR CNRS 7019), Institut Jean Barriol, Université de Lorraine, BP 239, Boulevard des Aiguillettes, Vandoeuvre-lès-Nancy 54506, France

## **Supporting Information (S.I.)**

**Chemicals used.** The following chemicals were used for the reactions as received: Ba rod (Alfa Aesar, 99.5%), Sr pieces (Sigma Aldrich, 99.5%), Ca granules (Sigma Aldrich, 99%), Pb ingot (Alfa Aesar, 99.99%), Sc arc cast pellet (Alfa Aesar, 99.9%), Y ingot (Alfa Aesar, 99.9%), Ru sponge (Alfa Aesar, 99.95%), Se powder (Sigma Aldrich, 99.5%), and Te pieces (Sigma Aldrich, 99.999%).

### **Attempts to synthesize analogues of Ba<sub>3</sub>ScTe<sub>5</sub>.**

We have tried various sealed-tube reactions to synthesize analogues of Ba<sub>3</sub>ScTe<sub>5</sub> by substituting the Ba atom with Sr, Ca, and Pb; trivalent Sc with Y and Ru; Te atom with Se. The heating profile of the synthesis of polycrystalline Ba<sub>3</sub>ScTe<sub>5</sub> was also used for these reactions. However, all these attempts failed, and only binary phases were obtained. The details of the reaction condition, reactants, and PXRD analysis are summarized in Table S1. The powder X-ray diffraction (PXRD) patterns of the reaction products of these reactions are depicted in Figure S1.

**Table S1. Details of Compositions and PXRD Analysis of Attempted Reactions for the Synthesis of Analogues of Ba<sub>3</sub>ScTe<sub>5</sub> Structure.**

Reaction code	Loaded composition	Reactants	PXRD analysis of product (Major phases)
R1	Ba <sub>3</sub> ScSe <sub>5</sub>	Ba (0.242 g, 1.76 mmol), Sc (0.0264 g, 0.587 mmol), Se (0.232 g, 2.936 mmol)	BaSe and BaSe <sub>3</sub>
R2	Ba <sub>3</sub> YTe <sub>5</sub>	Ba (0.181 g, 1.317 mmol), Y (0.039 g, 0.438 mmol), Te (0.280 g, 2.194 mmol)	BaTe and Y <sub>2</sub> Te <sub>3</sub>
R3	Sr <sub>3</sub> ScTe <sub>5</sub>	Sr (0.1389 g, 1.585 mmol), Te (0.3373 g, 2.643 mmol)	SrTe
R4	Sr <sub>3</sub> YTe <sub>5</sub>	Sr (0.133 g, 1.517 mmol), Y (0.0449 g, 0.505 mmol), Te (0.322 g, 2.523 mmol)	SrTe and Y <sub>2</sub> Te <sub>3</sub>
R5	Ca <sub>3</sub> ScTe <sub>5</sub>	Ca (0.075 g, 1.871 mmol), Sc (0.0280 g, 0.622 mmol), Te (0.397 g, 3.111 mmol)	CaTe
R6	Ca <sub>3</sub> YTe <sub>5</sub>	Ca (0.071 g, 1.771 mmol), Y (0.0525 g, 0.590 mmol), Te (0.377 g, 2.955 mmol)	CaTe
R7	Ba <sub>3</sub> RuTe <sub>5</sub>	Ba (0.179 g, 1.303 mmol), Ru (0.044 g, 0.435 mmol), Te (0.277 g, 2.171 mmol)	RuTe <sub>2</sub> and BaTe
R8	Pb <sub>3</sub> ScTe <sub>5</sub>	Pb (0.238 g, 1.150 mmol), Sc (0.017 g, 0.378 mmol), Te (0.245 g, 1.920 mmol)	PbTe
R9	Pb <sub>3</sub> YTe <sub>5</sub>	Pb (0.2305 g, 1.112 mmol), Y (0.039 g, 0.439 mmol), Te (0.237 g, 1.857 mmol)	PbTe

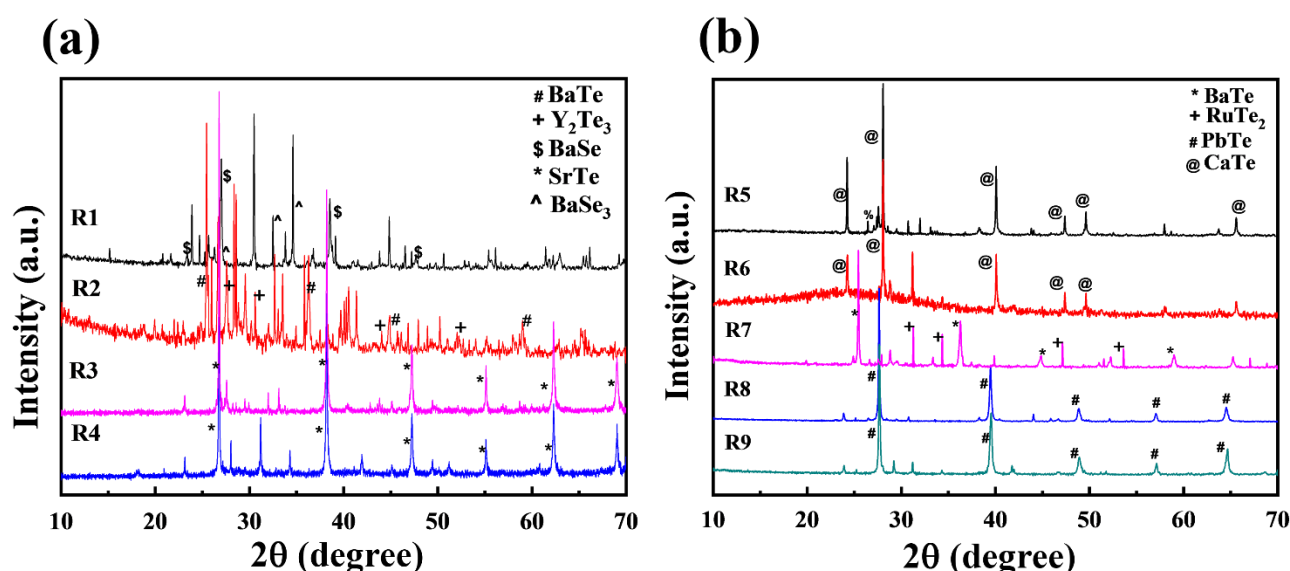


**Figure S1:** (a) Powder XRD patterns (reaction code R1-R4) and (b) (reaction code R4-R9) of product of reactions attempted to synthesize analogues of Ba<sub>3</sub>ScTe<sub>5</sub>.

**Raman Spectroscopy Measurement.** The Raman spectroscopy study of polycrystalline  $\text{Ba}_3\text{ScTe}_5$  was carried out at 298(2) K. A circular pellet which was made of polycrystalline  $\text{Ba}_3\text{ScTe}_5$  was placed under a Bruker SENTERRA II dispersive micro Raman spectrometer equipped with a confocal microscope to collect the data from 50 to 3500  $\text{cm}^{-1}$  at 4  $\text{cm}^{-1}$  resolution. An excitation wavelength of 532 nm was used to record the Raman spectrum.

Figure S2 shows the Raman spectrum of polycrystalline  $\text{Ba}_3\text{ScTe}_5$  that was collected at 298(2) K. Raman spectrum shows the presence of three intense bands at 90, 671.5, and 730  $\text{cm}^{-1}$ . There are other relatively less intense bands around 114, 185.5, 307, and 391  $\text{cm}^{-1}$ . The strong bands at 671.5  $\text{cm}^{-1}$  and 730  $\text{cm}^{-1}$  could be assigned to the Ba–Te bond stretching. These bands are close to the reported Ba–Te bands at 667  $\text{cm}^{-1}$  and 732  $\text{cm}^{-1}$  for  $\text{BaIn}_2\text{Te}_4$ .<sup>1</sup> Raman bond stretching frequencies of Sc–Te bonds are not reported in the literature. Hence, we could not assign bands corresponding to the Sc–Te bond stretching. Future theoretical work will be useful to interpret the observed Raman spectrum of  $\text{Ba}_3\text{ScTe}_5$  in detail.

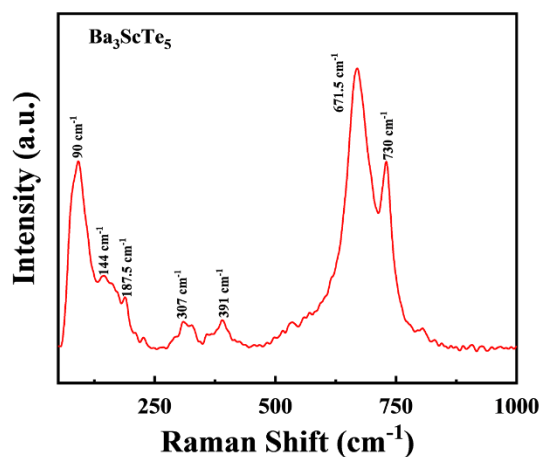


**Figure S2:** Raman spectrum of polycrystalline  $\text{Ba}_3\text{ScTe}_5$ .

**Table S2. Atomic Coordinates ( $\times 10^4$ ), Occupancies, and Equivalent Isotropic Displacement Parameters ( $\text{\AA}^2 \times 10^3$ ) for Modulated Structure of  $\text{Ba}_3\text{ScTe}_5$  at 100(2) K.**

Label	x	y	z	Occupancy	$U_{eq}^*$
Ba(1)	6143(2)	-8(2)	5000	1	11(1)
Ba(2)	-6157(2)	-8(2)	0	1	10(1)
Te(1)	2380(2)	2(2)	5000	1	6(1)
Te(2)	-2391(2)	3(2)	0	1	6(1)
Te(3)	6666.67	3333.33	2480(3)	1	7(1)
Te(4)	3333.33	-3333.33	-2480(3)	1	7(1)
Sc(1)	0	0	7463(9)	1	4(1)

\* $U_{eq}$  is defined as one third of the trace of the orthogonalized  $U_{ij}$  tensor.

**Table S3. Anisotropic Displacement Parameters ( $\text{\AA}^2 \times 10^3$ ) for  $\text{Ba}_3\text{ScTe}_5$  at 100(2) K.**

Label	$U_{11}$	$U_{22}$	$U_{33}$	$U_{12}$	$U_{13}$	$U_{23}$
Ba(1)	9(1)	7(1)	13(1)	2(1)	0	0
Ba(2)	10(1)	11(1)	12(1)	7(1)	0	0
Te(1)	6(1)	7(1)	5(1)	4(1)	0	0
Te(2)	7(1)	6(1)	5(1)	2(1)	0	0
Te(3)	6(1)	6(1)	9(1)	3(1)	0	0
Te(4)	6(1)	6(1)	9(1)	3(1)	0	0
Sc(1)	1(1)	1(1)	10(1)	1(1)	0	0

**Table S4. Fourier Components of The Displacive Modulation for Modulated Structure of Ba<sub>3</sub>ScTe<sub>5</sub> at 100(2) K.**

Label	Vector	Axis	cos displacement	sin displacement
Ba(1)	q(1)	x	0.0096(3)	0
Ba(1)	q(1)	y	0.0203(3)	0
Ba(1)	q(1)	z	0	0.0011(4)
Ba(2)	q(1)	x	-0.0107(3)	0
Ba(2)	q(1)	y	-0.0204(3)	0
Ba(2)	q(1)	z	0	-0.0012(4)
Te(1)	q(1)	x	-0.0046(4)	0
Te(1)	q(1)	y	-0.0086(4)	0
Te(1)	q(1)	z	0	-0.0002(4)
Te(2)	q(1)	x	0.0042(4)	0
Te(2)	q(1)	y	0.0089(4)	0
Te(2)	q(1)	z	0	0.0001(4)
Te(3)	q(1)	x	0	0
Te(3)	q(1)	y	0	0
Te(3)	q(1)	z	-0.0463(7)	-0.0034(5)
Te(4)	q(1)	x	0	0
Te(4)	q(1)	y	0	0
Te(4)	q(1)	z	-0.0472(7)	0.0035(5)
Sc(1)	q(1)	x	0	0
Sc(1)	q(1)	y	0	0
Sc(1)	q(1)	z	-0.002(3)	0.0000(6)

**Table S5. Interatomic Lengths Distributions [ $\text{\AA}$ ] for Modulated Structure of  $\text{Ba}_3\text{ScTe}_5$  at  $100(2)\text{ K}$ .**

Label	Average Distance	Minimum Distance	Maximum Distance
Ba(1)-Ba(2)#1	4.139(3)	4.120(4)	4.149(4)
Ba(1)-Ba(2)#2	4.139(3)	4.120(4)	4.149(4)
Ba(1)-Te(1)#3	3.412(4)	3.383(5)	3.444(5)
Ba(1)-Te(1)#4	3.406(6)	3.370(8)	3.445(8)
Ba(1)-Te(2)#1	3.724(3)	3.717(3)	3.729(3)
Ba(1)-Te(2)#2	3.724(3)	3.717(3)	3.729(3)
Ba(1)-Te(3)	3.599(4)	3.490(5)	3.692(5)
Ba(1)-Te(3)#5	3.598(4)	3.490(5)	3.692(5)
Ba(1)-Te(4)#6	3.588(3)	3.485(4)	3.674(4)
Ba(1)-Te(4)#7	3.586(3)	3.485(4)	3.674(4)
Ba(2)-Te(1)#8	3.728(3)	3.720(3)	3.732(3)
Ba(2)-Te(1)#9	3.728(3)	3.720(3)	3.732(3)
Ba(2)-Te(2)#10	3.404(4)	3.370(5)	3.441(5)
Ba(2)-Te(2)#11	3.409(6)	3.380(8)	3.440(8)
Ba(2)-Te(3)#9	3.588(3)	3.501(4)	3.658(4)
Ba(2)-Te(3)#12	3.588(3)	3.501(4)	3.658(4)
Ba(2)-Te(4)#9	3.576(4)	3.496(5)	3.640(5)
Ba(2)-Te(4)#12	3.576(4)	3.496(5)	3.640(5)
Te(1)-Sc(1)	2.937(8)	2.929(13)	2.946(13)
Te(1)-Sc(1)#5	2.937(9)	2.929(13)	2.946(13)
Te(2)-Sc(1)#13	2.978(9)	2.970(13)	2.987(13)
Te(2)-Sc(1)#5	2.978(9)	2.970(13)	2.987(13)
Te(3)-Te(3)#7	3.384(6)	2.834(7)	3.944(7)
Te(4)-Te(4)#7	3.395(7)	2.824(7)	3.955(7)
Sc(1)-Sc(1)#5	3.37(2)	3.35(2)	3.38(2)

Symmetry transformations used to generate equivalent atoms:

- (1)  $x_1+1, x_2, x_3, x_4$  (2)  $x_1+1, x_2, x_3+1, x_4$  (3)  $-x_2+1, x_1-x_2, x_3, x_4$  (4)  $-x_1+x_2+1, -x_1, x_3, x_4$  (5)  $x_1, x_2, -x_3+1, -x_4$  (6)  $x_1, x_2, x_3+1, x_4$  (7)  $x_1, x_2, -x_3, -x_4$  (8)  $x_1-1, x_2, x_3-1, x_4$  (9)  $x_1-1, x_2, x_3, x_4$  (10)  $-x_2-1, x_1-x_2, x_3, x_4$  (11)  $-x_1+x_2-1, -x_1, x_3, x_4$  (12)  $x_1-1, x_2, -x_3, -x_4$  (13)  $x_1, x_2, x_3-1, x_4$  (14)  $-x_2, x_1-x_2-1, x_3, x_4$  (15)  $-x_1+x_2+1, -x_1+1, x_3, x_4$  (16)  $-x_2, x_1-x_2+1, x_3, x_4$  (17)  $-x_1+x_2-1, -x_1-1, x_3, x_4$  (18)  $-x_2+1, x_1-x_2+1, x_3, x_4$  (19)  $-x_1+x_2, -x_1, x_3, x_4$  (20)  $-x_2, x_1-x_2-1, x_3-1, x_4$  (21)  $-x_1+x_2+1, -x_1, x_3-1, x_4$  (22)  $-x_2, x_1-x_2, x_3, x_4$  (23)  $-x_1+x_2, -x_1-1, x_3, x_4$  (24)  $-x_2, x_1-x_2, x_3+1, x_4$  (25)  $-x_1+x_2, -x_1, x_3+1, x_4$

**Table S6. Atomic Coordinates ( $\times 10^4$ ), Fourier Components of the Displacive Modulation ( $\times 10^4$ ), Occupancies, and Equivalent Isotropic Displacement Parameters ( $\text{\AA}^2 \times 10^3$ ) for  $\text{Ba}_3\text{ScTe}_5$  at 100(2) K.**

Atom	Wave	X	y	z	Occupancy	$U_{\text{eq}}$
Ba(1)	0	6143(2)	-8(2)	5000	1	11(1)
	sin,1	0	0	11(4)		
	cos,1	96(3)	203(3)	0		
Ba(2)	0	-6157(2)	-8(2)	0	1	10(1)
	sin,1	0	0	-12(4)		
	cos,1	-107(3)	-204(3)	0		
Te(1)	0	2380(2)	2(2)	5000	1	6(1)
	sin,1	0	0	-2(4)		
	cos,1	-46(4)	-86(4)	0		
Te(2)	0	-2391(2)	3(2)	0	1	6(1)
	sin,1	0	0	1(4)		
	cos,1	42(4)	89(4)	0		
Te(3)	0	6666.67	3333.33	2480(3)	1	7(1)
	sin,1	0	0	-34(5)		
	cos,1	0	0	-463(7)		
Te(4)	0	3333.33	-3333.33	-2480(3)	1	7(1)
	sin,1	0	0	35(5)		
	cos,1	0	0	-472(7)		
Sc(1)	0	0	0	7463(9)	1	4(1)
	sin,1	0	0	0(6)		
	cos,1	0	0	-20(30)		

**Table S7. Fourier Components of the Thermal Parameters Modulation ( $\text{\AA}^2 \times 10^3$ ) for  $\text{Ba}_3\text{ScTe}_5$  at 100(2) K.**

Atom	Wave	$U_{11}$	$U_{22}$	$U_{33}$	$U_{12}$	$U_{13}$	$U_{23}$
Ba(1)	0	9(1)	7(1)	13(1)	2(1)	0	0
	sin,1	0	0	0	0	-6(1)	-4(1)
	cos,1	5(2)	-2(2)	3(2)	1(2)	0	0
Ba(2)	0	10(1)	11(1)	12(1)	7(1)	0	0
	sin,1	0	0	0	0	-2(1)	3(1)
	cos,1	-5(2)	2(2)	-2(2)	-1(2)	0	0
Te(1)	0	6(1)	7(1)	5(1)	4(1)	0	0
	sin,1	0	0	0	0	-1(1)	1(1)
	cos,1	-1(2)	2(2)	0(2)	0(2)	0	0
Te(2)	0	7(1)	6(1)	5(1)	2(1)	0	0
	sin,1	0	0	0	0	-1(1)	0(1)
	cos,1	1(2)	-2(2)	0(2)	0(2)	0	0
Te(3)	0	6(1)	6(1)	9(1)	3(1)	0	0
	sin,1	0(2)	0(2)	17(3)	0(1)	0	0
	cos,1	1(1)	1(1)	-12(2)	0(1)	0	0
Te(4)	0	6(1)	6(1)	9(1)	3(1)	0	0
	sin,1	0(2)	0(2)	15(3)	0(1)	0	0
	cos,1	-1(1)	-1(1)	11(2)	0(1)	0	0
Sc(1)	0	1(1)	1(1)	10(1)	1(1)	0	0
	sin,1	0(4)	0(4)	1(10)	0(2)	0	0
	cos,1	0(1)	0(1)	-1(2)	0(1)	0	0

## Reference

1. Ishtiyak, M.; Jana, S.; Narayanswamy, S.; Nishad, A. K.; Panigrahi, G.; Bhattacharjee, P. P.; Prakash, J. Intrinsic extremely low thermal conductivity in  $\text{BaIn}_2\text{Te}_4$ : Synthesis, crystal structure, Raman spectroscopy, optical, and thermoelectric properties. *J. Alloys Compd.* **2019**, *802*, 385-393.